

Resolving Dynamic Properties of Polymers through Coarse-Grained Computational Studies

K. Michael Salerno,¹ Anupriya Agrawal,^{2,3} Dvora Perahia,³ and Gary S. Grest¹

¹*Sandia National Laboratories, Albuquerque, NM, 87185*

²*Department of Mechanical Engineering and Materials Science, Washington University, St. Louis, MO 63130*

³*Department of Chemistry, Clemson University, Clemson, SC 29634*

Coupled length and time scales determine the dynamic behavior of polymers and underlie their unique viscoelastic properties. To resolve the long-time dynamics it is imperative to determine which time and length scales must be correctly modeled. Here we probe the degree of coarse graining required to simultaneously retain significant atomistic details and access large length and time scales. The degree of coarse graining in turn sets the minimum length scale instrumental in defining polymer properties and dynamics. Using linear polyethylene as a model system, we probe how coarse graining scale affects the measured dynamics. Iterative Boltzmann inversion is used to derive coarse-grained potentials with 2-6 methylene groups per coarse-grained bead from a fully atomistic melt simulation. We show that atomistic detail is critical to capturing large scale dynamics. Using these models we simulate polyethylene melts for times over 500 μs to study the viscoelastic properties of well-entangled polymer chains.

Polymer properties depend on a wide range of coupled length and time scales, with unique viscoelastic properties stemming from interactions at the atomistic level. The need to probe polymers across time and length scales to capture polymer behavior makes probing dynamics, and particularly computational modeling, inherently challenging. With increasing molecular weight, polymer melts become highly entangled and the long-time diffusive regime becomes computationally inaccessible using atomistic simulations. In these systems the diffusive time scale increases with polymerization number N faster than N^3 , becoming greater than 10^{10} times larger than the shortest time scales even for modest molecular weight polymers. While it is clear that the largest length scales of polymer dynamics are controlled by entanglements, the shortest time and length scales required to resolve dynamic properties are not obvious. This knowledge is critical for developing models that can transpose atomistic details into the long time scales needed to model long, entangled polymer chains.

One path to overcoming this computational challenge is to coarse grain the polymer, reducing the number of degrees of freedom and increasing the fundamental time scale. The effectiveness of this process depends on retaining the smallest length scale essential to capturing the polymer dynamics. The process of coarse graining amounts to combining groups of atoms into pseudoatom beads and determining the bead interaction potentials [1, 2]. Simple models like the bead-spring model [3], capture characteristics described by scaling theories, but disregard atomistic details and cannot quantitatively describe properties like structure, local dynamics or densities. Immense efforts have been made to systematically coarse grain polymers and bridge the gap of time and length scales while retaining atomistic characteristics [4]. One critical issue underlying the coarse graining process is the degree to which a polymer can be coarse

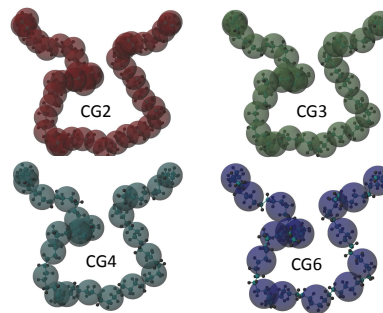


FIG. 1. A single $\text{C}_{96}\text{H}_{194}$ PE chain represented with increasing degree of coarse graining $\lambda = 2, 3, 4,$ and 6 methylene groups per CG bead. Bead diameter corresponds to the minimum in the nonbonded interaction for each CG model.

grained while still appropriately capturing polymer properties and dynamics [5]. The current study probes the effects of the degree of coarse graining of polymers on their dynamic and static properties.

With the vast efforts to coarse grain polymers, many models have emerged with differences in the number of atoms combined in each bead and the procedure for determining the interaction potentials. One of the most common coarse-grained (CG) models for polymers is the united atom (UA) model, which combines each CH_n group into a pseudoatom. The UA interaction parameters are determined phenomenologically to reproduce physical properties such as densities and critical temperatures [6–9]. Another model commonly used is the MARTINI model, which utilizes the same approach, matching bulk densities and compressibilities of short alkane chains at a larger scale of four CH_2 groups per CG bead [10]. More advanced methods such as force matching, iterative Boltzmann inversion, and optimized relative entropy [11–13] have recently been developed to incorporate atomistic

detail into the CG model. With these methods there is an open question as to the number of atoms to represent by a single bead and the effect of this coarse-graining scale on the measured properties of the system. One critical physics question remains unresolved: namely defining the shortest length scale in a polymer that is fundamental to the macroscopic dynamics and properties.[1, 3, 4, 6–13] Here, this issue is addressed through the development of CG models with increasing degree of coarse graining using iterative Boltzmann inversion. By examining how well these CG models describe both the static and dynamic properties of a polymer melt, using polyethylene (PE) as a model system, we probe this outstanding question. The backbone of PE consists of $-\text{CH}_2-$ methylene groups that provide a natural unit or scale for coarse graining. Though the chemical structure of PE is simple, it is a thermoplastic material useful in a large number of applications, with tunable mechanical properties determined by the degree of branching.

Polyethylene chains have previously been studied using CG models with beads of $\lambda = 3 - 48$ methylene groups per bead [14–19]. These studies were able to capture the radius of gyration as a function of molecular weight and the pair correlation function between CG beads. As most of these studies used a large degree of coarse graining ($\lambda \sim 20$) to study dynamical properties, an extra constraint was needed to prevent chains cutting through each other [20]. With this extra constraint, the mean squared displacement (MSD), stress autocorrelation function and shear viscosity of linear and branched PE [20–22] have been studied for long, entangled chains. However, these studies did not account for or study the effects of the coarse-graining degree λ on dynamic properties.

Here for the first time, we elucidate the effect of coarse-graining degree on the ability to capture both the structure and dynamics of PE. We are able to capture polymer chain dynamics for lengths up to $\text{C}_{1920}\text{H}_{3842}$ and time scales of $400 \mu\text{s}$ using models that accurately represent atomistic detail. Accessing large length and time scales allows us to measure quantities like the plateau modulus which depend on a hierarchy of length and time scales.

Coarse-grained beads shown in Fig. 1 represent λ methylene groups. We study $\lambda = 2, 3, 4$ and 6 and refer to these models as $\text{CG}\lambda$. We find that for surprisingly small λ the chains cross and diffuse rapidly, indicating that CG features directly link to macroscopic polymer motion. With this result, we further probed the CG6 model polymer including non-crossing constraints, and comparing with models with unconstrained dynamics.

The tabulated CG PE potentials were derived from a single fully-atomistic simulation of a melt of $\text{C}_{96}\text{H}_{194}$ PE chains at 500K. The study was then generalized to melts of $\text{C}_n\text{H}_{2n+2}$ with $n=96, 480$ for the fully atomistic model, and $n=96, 480, 960$ and 1920 at 500 K using the CG models. Atomistic simulations used a version of the Optimized Potentials for Liquid Simulations (OPLS)

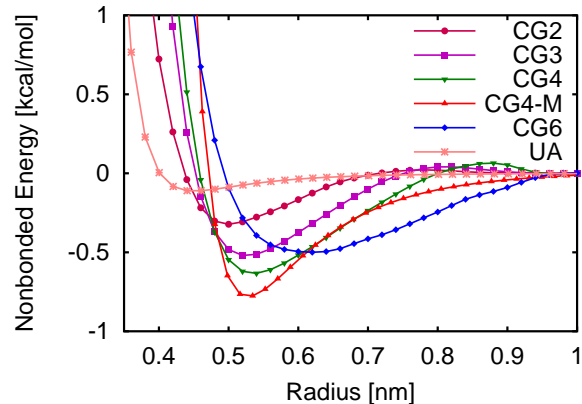


FIG. 2. Tabulated pair potential between CG beads. The UA and CG4-M potentials are included for comparison.

potential with modified dihedral coefficients that better reproduce the properties of long alkanes [24]. With this modified potential the mean squared radius of gyration $\langle R_g^2 \rangle$ and end to end distance $\langle R^2 \rangle$ match experimental values [25, 26] better than with original OPLS parameters [27]. For the $\text{CG}\lambda$ models, $\langle R^2 \rangle$ for $n=96$ chains is within 20% of the atomistic value, while $\langle R^2 \rangle$ for the MARTINI model is 50% too high. Static properties for different chain lengths are reported in the Supplement.

Tabulated CG angle and bond potentials were determined by Boltzmann inversion of the atomistic bond and angle distributions in Fig. S1. Torsion terms were omitted in all CG models, which may account for the shorter end to end distances listed in Table SI for the CG2 model. Tabulated nonbonded potentials were determined by iterative Boltzmann inversion [4]. The intermolecular radial distribution function $g(r)$ from the atomistic simulation, shown in Fig. S2, was used as the target for iteration of the nonbonded potentials shown in Fig. 2. Also shown are 6-12 Lennard Jones pair potentials for the united atom (UA) model of Yoon et al. [6], and the MARTINI (CG4-M) model [10]. The MARTINI parameter ϵ was reduced from 0.8365 kcal/mol to 0.803 kcal/mol to match the density $\rho = 0.72 \text{ g/cm}^3$ of atomistic simulations for $n = 96$ chains. For each CG model a pressure correction is applied to match the density $\rho = 0.72 \text{ g/cm}^3$ for $n=96$. The similarity in length and energy scales between the CG4 and CG4-M models is evident in Fig. 2. For each $\text{CG}\lambda$ model all beads identical interactions, however end beads have an extra hydrogen atom mass.

The CG6 model has a surprisingly large equilibrium bond distance relative to the bead diameter. Therefore a modified soft segmental repulsive potential [28] was added between CG beads to inhibit chain crossing. We used a segmental bead diameter of 0.5 nm . This scheme increases the pressure in our samples by about 80 atm

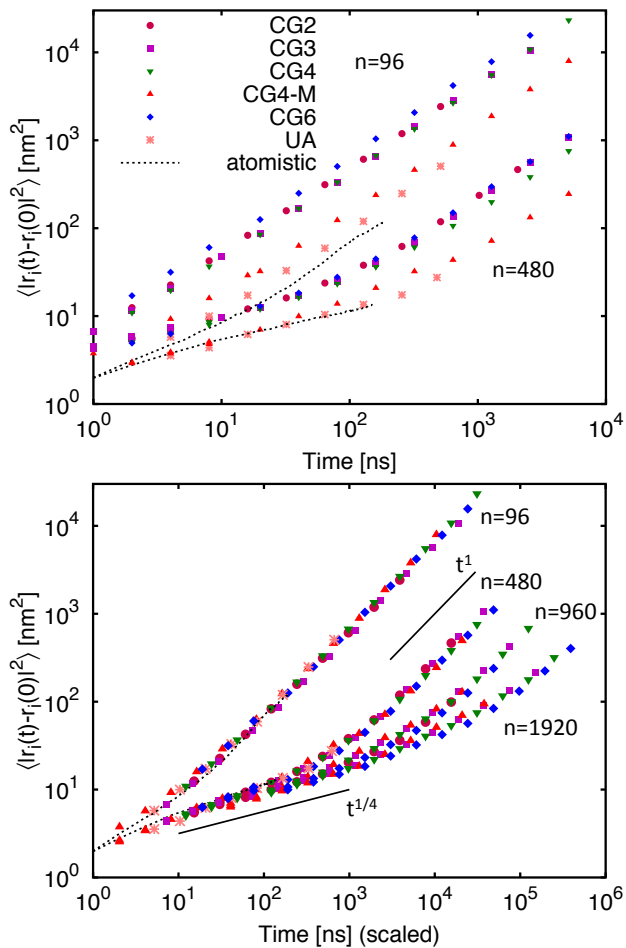


FIG. 3. (a) The MSD of the inner 24 $-\text{CH}_2-$ groups of each polymer chain at 500 K. (b) Same data as in (a), scaled by α . The solid lines represent the scaling predictions t^1 for the diffusive regime and $t^{1/4}$ for the reptation regime.

at fixed density compared to simulations with no constraint. We do not re-derive the potential including the soft segmental bead, however Fig. S3 shows that the non-crossing bead induces only small changes in $g(r)$ relative to a model with no constraint. By eliminating the finest degrees of freedom, CG models allow a significantly larger time step than atomistic models. We use a time step $\delta t = 20$ fs for the CG6, CG4 and CG4-M models, 10 fs for the CG3 model and 2 fs for the CG2 model, compared to 1 fs for the atomistic model.

Coarse graining reduces the number of degrees of freedom in a system, creating a smoother free-energy landscape compared with fully-atomistic simulations. This speedup can be addressed by including frictional and stochastic forces [15]. This approach allows large CG scales, however rigorously correct dissipation requires a sophisticated generalized Langevin kernel, and simplifications are usually employed [5]. It has been shown that for small λ CG models without added friction or stochastic forces can be employed, but CG dynamics are signif-

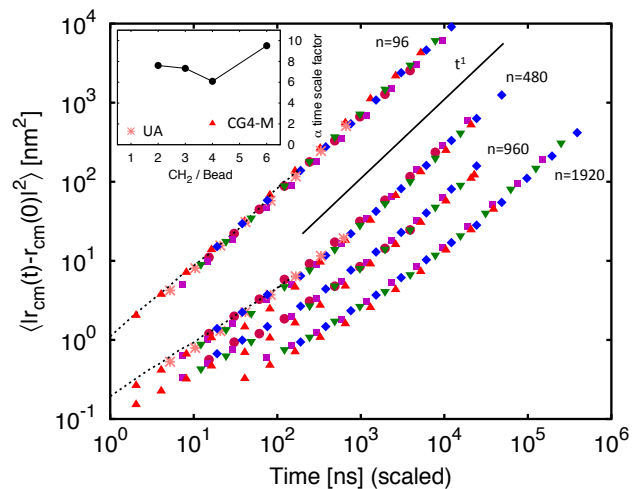


FIG. 4. MSD of center of mass scaled with the same α scale factor as the for the inner $-\text{CH}_2-$ groups in Fig. 3 (b). The solid line has slope t^1 . Inset: The alpha scale factor for different coarse-grained models and the UA and Martini models.

icantly faster than in atomistic simulations [29–36]. To determine the dynamic scaling factor of the CG models we compare the MSD of the inner 24 methylene groups (4, 6, 8 or 12 beads) for CG models and the inner 24 carbon atoms for atomistic simulations for $n=96$ and 480 as shown in Fig. 3 (a). The mobility of the chains in the CG models is larger than in atomistic simulations. By scaling the time for each of the CG models we create a single collapsed curve for each chain length for both the atomistic and CG data as shown in Fig.3 (b). Notably, a single scaling factor α is required to collapse atomistic and CG data for each model, independent of chain length. As seen in Fig. 3b the MSD has reached the diffusive regime where $\text{MSD} \sim t^1$ even for the longest chain length $n = 1920$. Over intermediate time scales, the chains show the expected $t^{1/4}$ scaling predicted by reptation theory [37]. These results demonstrate that one can capture long time and length scales with CG models while accounting for atomistic details.

The MSD of the center of mass was then measured to test the scaling factor α . Figure 4 shows the MSD of the chain center of mass for chain lengths $n=96, 480, 960,$ and 1920. These data have been scaled by the same α as the monomer MSD, producing an excellent collapse. The scale factor α as a function of CG model is shown inset in Fig. 4 along with α for the MARTINI [10] and UA [6] models. Our CG potentials have a much larger time scaling factor than the MARTINI and UA models, similar to the time-scaling factor found previously for PE for a single λ [30]. Values of α are also comparable to those found previously for polystyrene, modeled at a similar coarse-graining level [34]. The UA model has long been considered approximate to the fully-atomistic simulation and indeed is $\approx 40\%$ faster than fully-atomistic

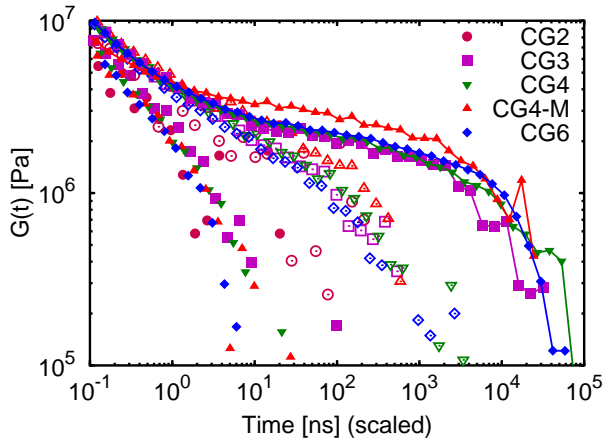


FIG. 5. Modulus $G(t)$ for each of the CG polymer models at 500K. Filled and open symbols represent the $n=96$ and $n=480$ chain length, respectively. Solid lines represent the $n=1920$ length, while $n=960$ chains are omitted for clarity.

simulations. Interestingly, the time scaling factor is not monotonic in CG level, with the CG2 and CG6 models exhibiting the largest speedup. The potential depths in Fig. 2, relate to the value of α , as described previously by Depa and Maranas [30].

The polymer entanglement mass M_e governs many properties of the polymer melt and provides information about chain mobility within the polymer mesh. Experimentally, $M_e = \rho RT/G_N^0$ is determined from the plateau modulus G_N^0 of the stress relaxation function $G(t)$ [25]. Experimental values for polyethylene are 1.6-2.5 MPa, corresponding to M_e of 1300-2000 g/mol [25, 26, 38, 39].

The relaxation modulus in each of our CG models was measured for the four different chain lengths via equilibrium stress correlations using the Green-Kubo relation $G(t) = (V/k_B T) \langle \sigma_{\alpha\beta}(t) \sigma_{\alpha\beta}(0) \rangle$ where $\sigma_{\alpha\beta}$ are the off-diagonal components xy , xz , and yz of stress. Figure 5 shows G_N^0 for each of the CG models for $n=96$ and 480 and for $\lambda \geq 3$ for $n = 1920$. The times for each model have been scaled by the corresponding value of α . Though it shows similar behavior, the UA model is omitted because the zero-pressure density is higher than the other models, making comparison difficult. The curves collapse for the short-time $t^{-1/2}$ regime, with longer, more entangled chains forming progressively more distinct plateau regions. The plateau modulus is measured as the value of the relaxation modulus in the plateau region, roughly between 20 and 600 ns. Using the longest chain length, $n = 1920$, the plateau modulus $G_N^0 = 2.2 \pm 0.3$ MPa for CG6, 2.1 ± 0.3 MPa for CG4 and 2.1 ± 0.7 MPa for CG3, all within the experimental range. For CG4-M G_N^0 is significantly higher $G_N^0 = 3.7 \pm 0.4$ MPa and does not agree with experimental values. Uncertainties are measured

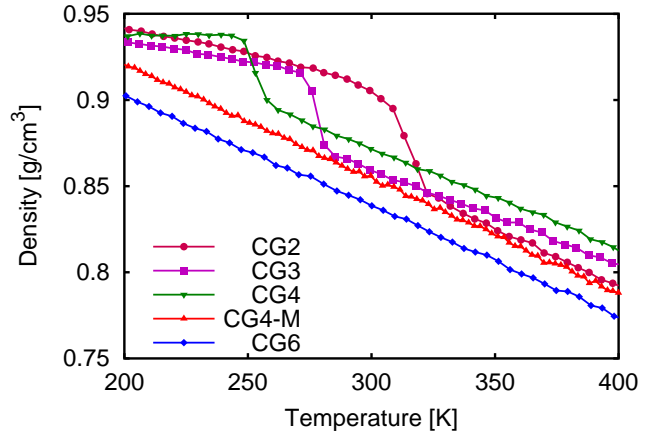


FIG. 6. Density versus temperature for the $n=96$ samples cooled at 1.4K/ns.

by dividing the datasets in two and measuring the variation in the plateau value. Similar plateau modulus values were found by Padding and Briels [20] for $n \leq 1000$ with $\lambda = 20$ model with a non-crossing constraint.

The thermal expansion coefficient is another way to assess the validity of the CG models. The linear thermal expansion coefficients for the $n=96$ samples in the temperature range from 495K to 480K are 5.0, 3.4, 3.5, 3.3, $3.4 \times 10^{-4} T^{-1}$ respectively for the CG2, CG3, CG4, CG4-M, and CG6 models, compared with $3.1 \times 10^{-4} T^{-1}$ for the atomistic model. Hence, all the CG models with $\lambda \geq 3$ agree with the atomistic thermal expansion.

Although one can derive CG potentials using multiple temperatures [40], our CG models are developed in the traditional way at a single temperature. Hence there is uncertainty about the validity of these models away from the chosen point [41]. Shown in Fig. 6 are temperature-density data for the CG models from 400K to 200K. For $\lambda \leq 4$, the curves show a pronounced density increase between 250K and 330K, corresponding to a semi-crystalline state. The CG6 model does not capture crystallinity and we expect that coarser models will not, either. Previous studies of bead-spring polymer models indicated that a commensurate bond length and bead diameter leads to crystallization [42]. The melting temperature for $n=96$ is about 400K, so crystallization occurs at a lower temperature than expected, yet observation of any semi-crystalline phase is remarkable. This surprising feature indicates that although our potentials are derived at 500K they may be useful away from this temperature.

Here we have shown that the smallest length scale needed in the hierarchy of length scales to correctly describe macroscopic behavior and properties is rather small, between 4 and 6 monomers. The CG4 model offers a speedup of more than four orders of magnitude over

atomistic simulations, which includes contributions from the time step δt , scale factor α , and $(3\lambda)^2$ reduction in the number of pairwise interactions. The speedup of the CG4 model is about three times faster than the CG3 model and is comparable the CG6 model. However because the CG4 model does not require a crossing constraint, we prefer this model. With this realized speedup polymers as long as $n = 1920$ can now be simulated for over 500 μs . Reaching this time scale allows probing some of the most unique and intrinsic properties of polymers including the plateau modulus and intermediate $t^{1/4}$ scaling in the mean squared displacement. From the computational viewpoint, the CG models developed significantly reduce the resources needed to study polymers for long times. Our results for the plateau modulus and diffusion dynamics show that without adding extra constraints the CG4 model captures the atomistic detail needed for correct dynamics from monomer to polymer scale.

AA and DP acknowledge financial support from Grant No. DE-SC007908 and an allotment of time on the Clemson University Palmetto cluster. This research used resources at the National Energy Research Scientific Computing Center, which is supported by the Office of Science of the U.S. Department of Energy under Contract DE-AC02-05CH11231. This work was supported by the Sandia Laboratory Directed Research and Development Program. Research was carried out in part, at the Center for Integrated Nanotechnologies, a U.S. Department of Energy, Office of Basic Energy Sciences user facility. Sandia National Laboratories is a multi-program laboratory managed and operated by Sandia Corporation, a wholly owned subsidiary of Lockheed Martin Corporation, for the U.S. Department of Energy's National Nuclear Security Administration under contract DE-AC04-94AL85000.

-
- [1] S. O. Nielsen, C. F. Lopez, G. Srinivas, and M. L. Klein, *J. Phys. Condens. Mat.* **16**, R481 (2004).
- [2] Y. Li, B. C. Abberton, M. Kröger, and W. K. Liu, *Polymers* **5**, 751 (2013).
- [3] K. Kremer and G. S. Grest, *J. Chem. Phys.* **92**, 5057 (1990).
- [4] F. Müller-Plathe, *Chem. Phys. Chem.* **3**, 754 (2002).
- [5] J. T. Padding and W. J. Briels, *Journal of Physics: Condensed Matter* **23**, 233101 (2011).
- [6] W. Paul, D. Y. Yoon, and G. D. Smith, *J. Chem. Phys.* **103**, 1702 (1995).
- [7] S. K. Nath, F. A. Escobedo, and J. J. de Pablo, *J. Chem. Phys.* **108**, 9905 (1998).
- [8] M. G. Martin and J. I. Siepmann, *J. Phys. Chem. B* **102**, 2569 (1998).
- [9] M. Mondello and G. S. Grest, *J. Chem. Phys.* **103**, 7156 (1995).
- [10] S. J. Marrink, H. J. Risselada, S. Yefimov, D. P. Tieleman, and A. H. de Vries, *J. Phys. Chem. B* **111**, 7812 (2007).
- [11] S. Izvekov and G. A. Voth, *J. Phys. Chem. B* **109**, 2469 (2005).
- [12] M. S. Shell, *J. Chem. Phys.* **129**, 144108 (2008).
- [13] V. Rühle and C. Junghans, *Macromol. Theor. Simul.* **20**, 472 (2011).
- [14] H. Fukunaga, J.-i. Takimoto, and M. Doi, *J. Chem. Phys.* **116**, 8183 (2002).
- [15] J. T. Padding and W. J. Briels, *J. Chem. Phys.* **115**, 2846 (2001).
- [16] H. S. Ashbaugh, H. A. Patel, S. K. Kumar, and S. Garde, *J. Chem. Phys.* **122**, 104908 (2005).
- [17] X. Guerrault, B. Rousseau, and J. Farago, *J. Chem. Phys.* **121**, 6538 (2004).
- [18] L.-J. Chen, H.-J. Qian, Z.-Y. Lu, Z.-S. Li, and C.-C. Sun, *J. Phys. Chem. B* **110**, 24093 (2006).
- [19] D. Curcó and C. Alemán, *Chem. Phys. Lett.* **436**, 189 (2007).
- [20] J. T. Padding and W. J. Briels, *J. Chem. Phys.* **117**, 925 (2002).
- [21] J. T. Padding and W. J. Briels, *J. Chem. Phys.* **118**, 10276 (2003).
- [22] L. Liu, J. T. Padding, W. K. den Otter, and W. J. Briels, *J. Chem. Phys.* **138**, 244912 (2013).
- [23] See Supplemental Material [url], which includes Refs. [43–45].
- [24] S. W. I. Siu, K. Pluhackova, and R. A. Böckmann, *J. Chem. Theory Comput.* **8**, 1459 (2012).
- [25] L. J. Fetters, D. J. Lohse, S. T. Milner, and W. W. Graessley, *Macromolecules* **32**, 6847 (1999).
- [26] L. J. Fetters, D. J. Lohse, and W. W. Graessley, *J. Polym. Sci. Pol. Phys.* **37**, 1023 (1999).
- [27] W. L. Jorgensen, D. S. Maxwell, and J. Tirado-Rives, *J. Am. Chem. Soc.* **118**, 11225 (1996).
- [28] T. W. Sirk, Y. R. Slizoberg, J. K. Brennan, M. Lisal, and J. W. Andzelm, *J. Chem. Phys.* **136**, 134903 (2012).
- [29] P. Depa, C. Chen, and J. K. Maranas, *J. Chem. Phys.* **134**, 014903 (2011).
- [30] P. K. Depa and J. K. Maranas, *J. Chem. Phys.* **123**, 094901 (2005).
- [31] I. Y. Lyubimov and M. G. Guenza, *J. Chem. Phys.* **138**, 12A546 (2013).
- [32] I. Y. Lyubimov, J. McCarty, A. Clark, and M. G. Guenza, *J. Chem. Phys.* **132**, 224903 (2010).
- [33] V. Harmandaris, *Korea-Aust. Rheol. J.* **26**, 15 (2014).
- [34] V. A. Harmandaris and K. Kremer, *Soft Matter* **5**, 3920 (2009).
- [35] D. Fritz, K. Koschke, V. A. Harmandaris, N. F. A. van der Vegt, and K. Kremer, *Phys. Chem. Chem. Phys.* **13**, 10412 (2011).
- [36] B. Hess, S. Leon, N. van der Vegt, and K. Kremer, *Soft Matter* **2**, 409 (2006).
- [37] P. G. de Gennes, *J. Chem. Phys.* **72**, 4756 (1980).
- [38] J. F. Vega, S. Rastogi, G. W. M. Peters, and H. E. H. Meijer, *J. Rheol.* **48**, 663 (2004).
- [39] V. R. Raju, G. G. Smith, G. Marin, J. R. Knox, and W. W. Graessley, *J. Polym. Sci. Pol. Phys.* **17**, 1183 (1979).
- [40] T. C. Moore, C. R. Iacovella, and C. McCabe, *J. Chem. Phys.* **140**, 224104 (2014).
- [41] P. Carbone, H. A. K. Varzaneh, X. Chen, and F. Müller-Plathe, *J. Chem. Phys.* **128**, 064904 (2008).
- [42] R. S. Hoy and N. C. Karayiannis, *Phys. Rev. E* **88**, 012601 (2013).

- [43] M. Tuckerman, B. J. Berne, and G. J. Martyna, *J. Chem. Phys.* **97**, 1990 (1992).
- [44] R. E. Isele-Holder, W. Mitchell, and A. E. Ismail, *J. Chem. Phys.* **137**, 174107 (2012).
- [45] S. Plimpton, *J. Comput. Phys.* **117**, 1 (1995).